Probability of Flood-Induced Overtopping of Barriers in Watershed-Reservoir-Dam Systems

Luis A. de Béjar, M.ASCE[1]

Abstract: An engineering methodology is developed to build hazard curves to evaluate the probability of flood-induced overtopping of barriers in watershed-reservoir-dam systems. The probable maximum precipitation in the watershed under consideration and its distribution in time during the acting storm is estimated. Considering the effects of the local geology, soil, topography, and land use, a random representation of the storm hourly rain is translated into effective runoff, including losses due to evaporation, interception, and surface retention. The uncertainty in the hydrological characteristics of the drainage basin is captured by a random time to concentration. Random hourly unit graphs are constructed analytically for a convex watershed and convoluted with the storm time-history to result in the random hydrograph for the inflow flood into the reservoir of the dam system. Flood routing through the reservoir is then computed with or without noise in the model. The deterministic path leads to a hydrograph for the water level at the barrier upstream face. The stochastic path evaluates through simulation the probability density function of variates (at discrete times) of the nonstationary random process of this pool level. The characterization of the reservoir-pool maxima allows the estimation of the probability of barrier overtopping. **DOI: 10.1061/(ASCE)HE .1943-5584.0000361.**

CE Database subject headings: Hydrographs; Watersheds; Routing; Reservoirs; Floods; Wave overtopping; Barriers.

Author keywords: Hyetographs; Watershed hydrograph; Routing through a reservoir; Random reservoir capacity; Reservoir hydrograph; Flood-induced overtopping; Hazard curves.

Introduction

During the last decade, the U.S. Army Corps of Engineers has embarked in a research program to produce engineering tools to assist analysts and decision makers in evaluating the components of dam and levee portfolios exposed to natural hazards. Risk-based approaches to barrier safety assessment provide a rational means to allocate limited resources to required maintenance and retrofit projects. This investigation is a contribution to the research effort concerning the overtopping of barriers under flood in overall watershed-reservoir-dam systems subjected to extreme water-input events.

A realistic mathematical model for an inherently random watershed-reservoir-dam system must involve the probabilistic representation of some of its components. A closed-form solution for the response of the system to a given water-input event proves difficult to obtain, if not impossible, in view of the complexity and ultimate nonlinearity of the governing formulations. Consequently, to arrive at useful conclusions in the study of a given system, the analyst must conduct a large number of numerical simulations of possible realizations. For this procedure to be practical in exercises of risk assessment of spillways and dam nonoverflow monoliths under flood hazard, the associated mathematical model must be both effective and economical. This paper introduces an engineering model to evaluate the probability of flood-induced overtopping of barriers in watershed-reservoir-dam systems by means of mathematical simulations while capturing the essential characteristics of the physical system.

Hyetographs for a given basin are built by inserting rational elements into the current state of practice [U.S. Bureau of Reclamation (USBR) 1976, 1977]. A simplified representation of the watershed is introduced at the level of the fundamental unit graph. All subsequent compositions are mathematically rigorous, leading to a convolution integral for a rational watershed-output hydrograph. The reservoir is represented by a nonlinear ordinary differential equation formulated on the basis of the principle of continuity and on the assumption of a convex reservoir. The spillway discharge is modeled by using the von Mises semiempirical formula for a wide-weir flow (Street et al. 1996). Deterministic interpretations of the model provide insight into the physical behavior of the system through parametric studies on the occurrence of hydrograph peaks, response spectra, and residual reservoir pools. Stochastic interpretations of the model provide insight into the resulting response random processes and the associated hazard curves necessary for subsequent evaluations of the probabilities of occurrence of multiple failure modes, e.g., overtopping, overstressing, overturning, and sliding instability (Ellingwood 1995, de Béjar 1999).

The relevant features of the USBR-recommended procedure for input-event characterization are retained in this model. Soil Conservation Service (SCS) maps of probable maximum precipitation (PMP) during extreme storms are adopted as mean values of extreme-value distributions (Miller and Clark 1960). USBR empirical factors for the determination of excess rain are directly implemented, as are the SCS charts for cover and land use complex coefficients.

To focus on the effect of a few essential factors on the system response, and to keep the formulation sufficiently simple to promote physical insight, only two basic random variables are

[1]Research Structural Engineer, U.S. Army Engineer Research and Development Center, Vicksburg, MS 39180-6199. E-mail: Luis.A .DeBejar@erdc.usace.army.mil

Note. This manuscript was submitted on May 27, 2009; approved on December 27, 2010; published online on December 29, 2010. Discussion period open until February 1, 2012; separate discussions must be submitted for individual papers. This paper is part of the ***Journal of Hydrologic Engineering***, Vol. 16, No. 9, September 1, 2011. ©ASCE, ISSN 1084-0699/2011/9-0–0/$25.00.

Report Documentation Page

Form Approved
OMB No. 0704-0188

1. REPORT DATE	2. REPORT TYPE	3. DATES COVERED
SEP 2011		**00-00-2011 to 00-00-2011**

4. TITLE AND SUBTITLE	5a. CONTRACT NUMBER
Probability Of Flood-Induced Overtopping Of Barriers In Watershed-Reservoir-Dam Systems	5b. GRANT NUMBER
	5c. PROGRAM ELEMENT NUMBER
6. AUTHOR(S)	5d. PROJECT NUMBER
	5e. TASK NUMBER
	5f. WORK UNIT NUMBER
7. PERFORMING ORGANIZATION NAME(S) AND ADDRESS(ES) **U.S. Army Engineer Research and Development Center,Research Structural Engineer,Vicksburg,MS,39180**	8. PERFORMING ORGANIZATION REPORT NUMBER
9. SPONSORING/MONITORING AGENCY NAME(S) AND ADDRESS(ES)	10. SPONSOR/MONITOR'S ACRONYM(S)
	11. SPONSOR/MONITOR'S REPORT NUMBER(S)

12. DISTRIBUTION/AVAILABILITY STATEMENT
Approved for public release; distribution unlimited

13. SUPPLEMENTARY NOTES
Journal Of Hydrologic Engineering,September 2011

14. ABSTRACT

An engineering methodology is developed to build hazard curves to evaluate the probability of flood-induced overtopping of barriers in watershed-reservoir-dam systems. The probable maximum precipitation in the watershed under consideration and its distribution in time during the acting storm is estimated. Considering the effects of the local geology, soil, topography, and land use, a random representation of the storm hourly rain is translated into effective runoff, including losses due to evaporation, interception, and surface retention. The uncertainty in the hydrological characteristics of the drainage basin is captured by a random time to concentration. Random hourly unit graphs are constructed analytically for a convex watershed and convoluted with the storm time-history to result in the random hydrograph for the inflow flood into the reservoir of the dam system. Flood routing through the reservoir is then computed with or without noise in the model. The deterministic path leads to a hydrograph for the water level at the barrier upstream face. The stochastic path evaluates through simulation the probability density function of variates (at discrete times) of the nonstationary random process of this pool level. The characterization of the reservoir-pool maxima allows the estimation of the probability of barrier overtopping

15. SUBJECT TERMS

16. SECURITY CLASSIFICATION OF:			17. LIMITATION OF ABSTRACT	18. NUMBER OF PAGES	19a. NAME OF RESPONSIBLE PERSON
a. REPORT **unclassified**	b. ABSTRACT **unclassified**	c. THIS PAGE **unclassified**	**Same as Report (SAR)**	**13**	

included in the watershed stochastic model: (1) the storm magnitude, and (2) the watershed characteristic centroidal lag time. The study of the random process representing the variation in reservoir pool in response to the water-input event is conducted with and without the presence of noise in the reservoir for comparison among the resulting hazard curves.

Analytical Models

The physical system to be modeled consists of three major components (Fig. 1): the watershed or drainage basin; the reservoir or excess-rain storage; and the spillway-dam structure, generally equipped with a gate system for flood control and evacuation.

The U.S. Weather Bureau, in collaboration with the U.S. Army Corps of Engineers, has developed empirical charts to estimate the historical 6-h, 10 mi^2 PMP attributable to a uniform storm on such a point within the basin area (USBR 1976, 1977). The proper chart to be applied depends on the specific geographical location of the project site. The charts are built for U.S. zones either east or west of the 105° meridian. To be specific, the model developed in this research applies to U.S. watersheds east of the 105° meridian, but a parallel development may just as easily be formulated for U.S. western watersheds.

Subsequently, the point-storm PMP is scaled up on the basis of empirical charts for the size of the specific drainage area under consideration and for several values of storm duration in order to estimate upper bounds of cumulative total rain falling uniformly over the watershed. These estimates of precipitation are taken as the known PMP distribution in time in the deterministic formulations, or as mean values of the extreme-value distribution of the largest values, Type I (Gumbel distribution) in the probabilistic formulations (Benjamin and Cornell 1970).

The watershed represents the first filter in the system. A substantial portion of the falling rain is lost because of a variety of factors. Among the main factors contributing to rain loss are (1) evaporation and transpiration; (2) retention by vegetation and by topographic details of the terrain (including minor ponds); and (3) surficial infiltration and deep percolation, depending on the type of soil cover and the geological characteristics of the region. The difference between total rain and losses other than those from rapid drainage water flowing through cover soil is the excess rain, defined as runoff in this investigation.

Runoff is evacuated relatively rapidly from the watershed through open channels and rivers that lead to the reservoir entrance (Point B in the schematic representation in Fig. 1), where the runoff flow $Q(t)$ can be measured (Fig. 2).

The storm total rain is translated into incremental runoff using semiempirical transformations (Miller and Clark 1960) that include consideration of a complex index to classify the watershed according to the cover soil and the land use. This piecewise-constant effective water-input history is applied to the watershed hourly during the first 6 h of storm, and thereafter in incremental time intervals of 6, 12, and 24 h., respectively. However, the order of hourly precipitation during the first 6 h of the storm cannot be predicted. Therefore, in this model, the specific order of the rain steps for a given storm is subjected to aleatory permutation, whether the representation is deterministic or not.

Fig. 2 shows the longitudinal section of the analytical model for the reservoir component in the system. The input flow $Q(t)$ represents the response of the watershed to the water-input event. The spillway outflow, $q[h(t), c]$, at the opposite end of the reservoir (see Fig. 3) depends on the discharge coefficient c, which in turn is a function of the weir elevation z, and of the reservoir elevation $h(t)$ itself, giving rise to a highly nonlinear governing differential equation for the response. The reservoir water level over the spillway crest $h(t)$ is directly related to the storm-water storage and

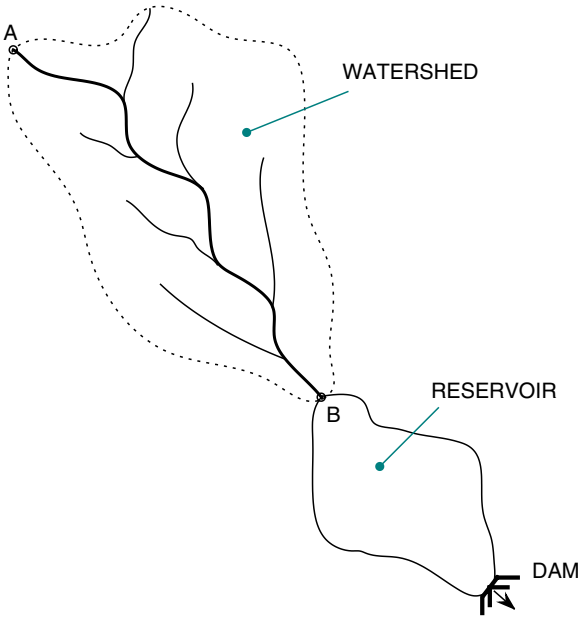

Fig. 1. Schematic plan view of a watershed-reservoir-dam system

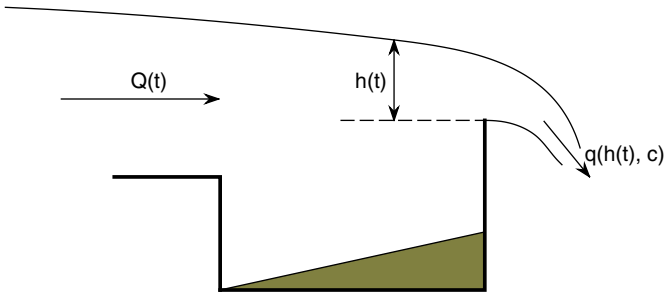

Fig. 2. Longitudinal section of analytical model of a reservoir

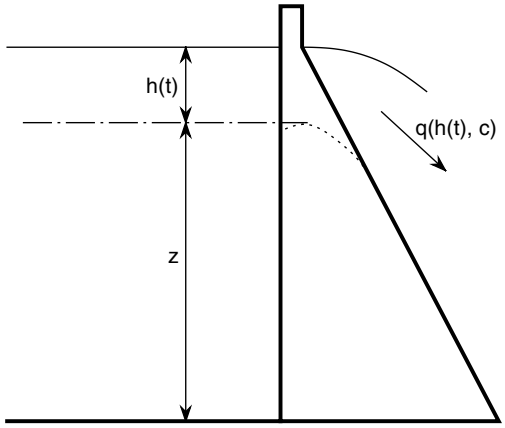

Fig. 3. Transverse section of analytical model of nonoverflow dam monolith (spillway crest is schematically represented by the dotted line)

represents the hazard on the dam structure whose safety is to be evaluated against various potential modes of failure, e.g., overtopping of nonoverflow barriers. For simplicity, the pool level at the beginning of the storm is considered to be that of the spillway crest, but any other convenient datum may be arbitrarily defined.

The model differs from the real reservoir by the fact that the bottom of the reservoir may be randomly covered with sediments over time, and also that topographical surveys are imperfect, particularly in the vicinity of the boundary of the reservoir. The corresponding effects on the governing differential equation for the reservoir response are optionally included in the probabilistic version of the model by adding a Gaussian noise component to the input random process.

Convex Unit Graph

The convex model for the response of a watershed to a water-input event is based on the principle of continuity and on a postulated linear relationship between the response flow $q[h(t), c]$ and the watershed storage $S(t)$. When the storm inflow is constant, the governing differential equation may be expressed as (Dingman 1994)

$$\frac{dS}{dt} + \left(\frac{1}{T^*}\right) \cdot S = \omega_0 \tag{1}$$

where T^* = centroidal lag between the inflow and outflow hydrographs, a constant characteristic of the watershed. The solution to this equation under zero initial conditions is

$$q(t) = \frac{S(t)}{T^*} = \omega_0 \cdot (1 - e^{-k^* \cdot t}), \qquad 0 \le t \le t_\omega \tag{2}$$

where $k^* = 1/T^*$. This result indicates that the output response approaches asymptotically the inflow ω_0 as far as the termination of the water-input event t_ω. At this time the recession limb of the response starts an exponential decay toward the zero-flow value. This indicates that the time to concentration of the model tends to infinity, similar to the time to concentration of a real watershed. The recession limb of the response is given by

$$q(t) = q_{pk} \cdot e^{-k^* \cdot (t - t_\omega)}, \qquad t > t_\omega \tag{3}$$

where $q_{pk} = q(t_\omega)$ = maximum value of the outflow. The only parameter characterizing the response is T^*, which may be estimated as

$$T^* = \frac{L_r}{U_w} \tag{4}$$

where L_r = length of the longest reach in the drainage basin (distance between Points A and B along the stream in Fig. 1); and U_w = velocity of propagation of the flood wave.

The convex unit graph is defined in this investigation as the outflow response of the watershed to a constant-rate water-input event with a total volume of unit value (i.e., a volume of rain with 1 cm of depth and uniformly distributed over the whole drainage area). The duration of this constant-rate water-input event is the unit period, which in this model is set as 1 h.

Watershed Response Hydrograph

The watershed response hydrograph is obtained by superposition in time of the scaled hydrographs corresponding to the actual incremental effective rain volumes (expressed in centimeters of rain uniformly distributed over the whole watershed area). Analytically, this procedure can be generalized by considering the response to a unit-volume input rain concentrated at the origin of time. In other words, the watershed output response is in this case the unit-impulse response function $u(t)$, as the input rain is a Dirac delta function at the origin of time, i.e., a zero-duration unit-volume rain at $t = 0$. In this case, the governing differential equation for the watershed becomes

$$T^* \cdot \frac{du}{dt} + u(t) = \delta(t) \tag{5}$$

with initial condition $u(0) = 0$. The general solution of this equation is

$$u(t) = A \cdot e^{-k^* \cdot t} \tag{6}$$

The constant of integration A may be obtained by integrating Eq. (5) over the infinitesimal time interval $(-\varepsilon, +\varepsilon)$, and taking the limit as $\varepsilon \to 0$, to obtain the unit-impulse response function as

$$u(t) = k^* \cdot e^{-k^* \cdot t}, \qquad t > 0 \tag{7}$$

The watershed response hydrograph to an inflow with the rate of rain $r(t)$ may be obtained by superposition in the time domain and is given by the convolution integral

$$q(t) = \int_{0^+}^{t} r(t - \tau) \cdot u(\tau) \cdot d\tau, \qquad t > 0 \tag{8}$$

In fact, the response to $r(t) = \omega_0$ = constant may also be obtained as the expressions in Eqs. (2) and (3) by direct evaluation of Eq. (8).

Fig. 4 shows a family of these responses for a storm with magnitude $\omega = 1$ dkm^3/s acting during 4 h. The parameter T^* for the family of curves vary from a value $T^* = 25$ h. (a slow-evacuation watershed) to a value $T^* = 2.5$ h. (a rapid-evacuation watershed). The slow watersheds have smaller peak values of outflow and larger residual flows at the end of the period under consideration (10 h). On the other hand, the rapid watersheds often get almost to the asymptotic value ω_0 within the storm duration and rapidly decay toward zero residual flow upon storm termination.

The procedure described up to this point to construct the inflow design flood hydrograph into the reservoir (i.e., the watershed outflow hydrograph) is shown in the flow diagram in Fig. 5. This schematic structure is followed in both the deterministic and the probabilistic versions of the model under construction. Again, the probabilistic model concentrates on the effects of a random

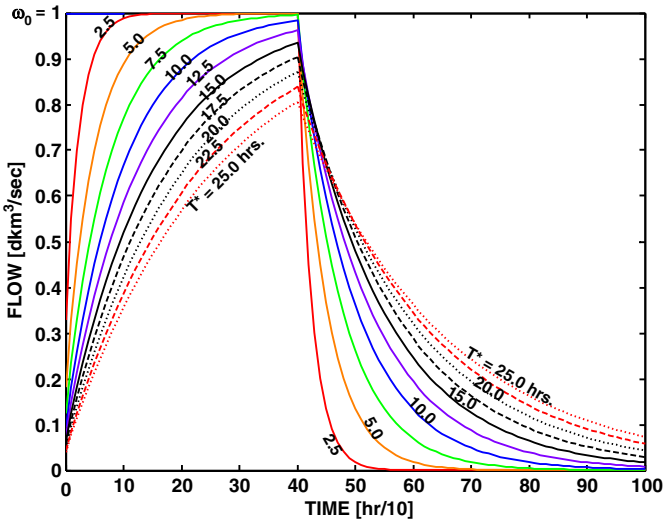

Fig. 4. Family of convex-watershed responses to a uniform runoff flow ω_o acting during a finite time interval (4 h); curves in the set are characterized by the centroidal lag time T^*

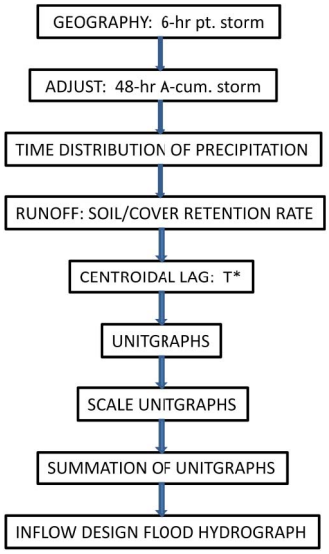

Fig. 5. Procedure to construct an inflow-flood hydrograph for a typical reservoir

water-input event magnitude and of a random watershed centroidal lag T^*.

Deterministic Model

An examination of the physical quantities entering the deterministic formulation for the response of the watershed-reservoir-dam system to a water-input event and its sensitivity to variations in those quantities proves to be insightful in revealing the fundamental nature of the relations involved.

Watershed Routing

In this model, the response of the watershed-reservoir-dam system is followed for a time interval of 60 h after the beginning of the storm, which is assumed to last 48 h. The subscript $i = 1, 2, \ldots, 6$ refers to the first six 1-h intervals; $i = 7, 8, 9$ refers to the time intervals following the first 6 h of storm duration with time lengths of 6, 12, and 24 h, respectively; and $i = 10$ refers to the last 12 h of rain-free history of response.

The procedure to determine the incremental runoff during each of these intervals follows the standard recommendations of practice (Miller and Clark 1960; USBR 1976, 1977). According to the geographical location and extension of the watershed, the 6-h point PMP is distributed in time and expressed as the accumulative rain fall in the actual-size watershed at the end of each of the intervals described previously (r_i, $i = 6, \ldots, 9$). This distribution may be expressed as

$$r_i + 5 = a_i \cdot \rho, \qquad i = 1, .., 4 \tag{9}$$

where ρ = 6-h point PMP; and a_i = empirical coefficient. Likewise, the accumulative rainfall at the end of each of the first six 1-h intervals may be expressed as

$$r_i = b_i \cdot r_6, \qquad i = 1, .., 6 \tag{10}$$

where r_6 = accumulative total rain at the end of 6 h of storm, as provided by Eq. (9); and b_i = empirical coefficient. Therefore, the incremental total rain corresponding to each of the first 1-h intervals is given by

$$\Delta r_1 = r_1, \qquad \Delta r_i = r_i - r_{i-1}, \qquad i = 2, \ldots, 6 \tag{11}$$

Again, the order of these first six 1-h incremental contributions to the total precipitation cannot be predicted, and they are given an aleatory permutation, after which the accumulative total rain is recalculated according to

$$r_1 = \Delta r_1, \qquad r_i = r_{i-1} + \Delta r_i, \qquad i = 2, \ldots, 9 \tag{12}$$

Next, the accumulative and incremental effective precipitations (direct runoff) are calculated. These calculations require the estimation of the local hydrologic soil-cover complex number (S) according to the soil-series classification and the combined land use at the site (USBR 1976, 1977), modified according to the antecedent conditions. The U.S. SCS (Miller and Clark 1960) recommends the use of the following fit to estimate runoff (based on numerous statistical studies and assuming the initial abstraction as $I_a = 0.2 \cdot S$):

$$p_i = \frac{(r_i - 0.2 \cdot S)^2}{r_i + 0.8 \cdot S}, \qquad i = 1, .., 9 \tag{13}$$

where p_i = accumulative runoff at the end of the ith time interval; and

$$\Delta p_1 = p_1, \qquad \Delta p_i = p_i - p_{i-1}, \qquad i = 2, \ldots, 9 \tag{14}$$

where Δp_i = incremental runoff corresponding to the ith time interval.

There is a physical lower bound for the hourly loss during each interval (Miller and Clark 1960). In this model, the hourly loss is not allowed to be less than 1.27 mm. Upon insertion of this minimum value, the incremental runoff is recalculated for each interval as

$$\Delta p_i^* = \Delta r_i - \Delta L_i, \qquad i = 1, ..9 \tag{15}$$

and

$$p_1^* = \Delta p_1^*, \qquad p_i^* = \Delta p_i^* + p_{i-1}, \qquad i = 2, \ldots, 9 \tag{16}$$

where ΔL_i = total loss corresponding to the ith interval; and symbols with an attached asterisk correspond to the recalculated quantities.

The watershed routing is completed using the convolution integral in Eq. (8) reformulated for computational analysis. When the input effective precipitation is represented by a piecewise constant function, Eq. (8) provides the watershed response upon water-input event termination as

$$q(t) = \sum_{i=1}^{9} q_{pk,i} \cdot e^{-k^* \cdot (t - t_i)}, \qquad t > t_\omega$$

in other words

$$q(t) = \sum_{i=1}^{9} (\text{Recess})_i \tag{17}$$

where $(\text{Recess})_i$ = contribution of the recession limb of the response to the ith increment of direct runoff when acting alone during the time interval ending at t_i; and $q_{pk,i}$ = corresponding maximum response [as in Eq. (3)]; and the following watershed response for times within the duration of the water-input event:

$$q(t) = \sum_{i=1}^{j} (\text{Recess})_i + p_{j+1} \cdot (1 - e^{-k^* \cdot (t - t_j)}),$$
$$t_j < t \le t_\omega, \qquad j \ge 0 \tag{18}$$

when the response is evaluated within the $(j + 1)$th interval, and the initial time is zero.

Reservoir Routing

The outflow from the routing of rain fall through the watershed represents the inflow for the reservoir component. Based on the principle of continuity, the governing differential equation for the reservoir routing in terms of the pool at the upstream face of the dam, $h(t)$, is given by (Jiang 1998)

$$\frac{dh}{dt} = \frac{Q(t) - q[h(t), c]}{G[h(t)]} \tag{19}$$

where $Q(t)$ = inflow from the watershed given by Eqs. (17) and (18); $q[h(t), c]$ = outflow through the spillway weir; c = corresponding discharge coefficient; and $G(h)$ = gradient of variation of the reservoir storage as a function of the reservoir pool. Other outlet works may be included in $q[h(t), c]$, if present. In this model, for simplicity, only a rectangular spillway weir is considered. The outflow through a rectangular weir may be estimated by (Street et al. 1996)

$$q[h(t), c] = \frac{2}{3} \cdot b \cdot c \cdot \sqrt{2g} \cdot h(t)^{3/2} \tag{20}$$

where b = weir length; c = discharge coefficient; and g = acceleration of gravity. Von Mises has developed a simple semiempirical expression for the coefficient of discharge as (Olson 1961)

$$c = 0.611 + 0.075 \cdot \frac{h(t)}{z} \tag{21}$$

where z = height of the spillway crest over the reservoir bottom (Fig. 3).

The reservoir storage may be regressed empirically as a quadratic function of the reservoir pool (Jiang 1998), leading to a linear fit for the corresponding gradient, which may be expressed as

$$G(h) = \alpha + \beta \cdot h \tag{22}$$

where α and β = empirical coefficients for the reservoir considered, given in consistent units, i.e., α [m^3/m] and β [m^2/m]. Inserting Eqs. (17), (18), and (20)–(22) into Eq. (19) leads to a nonlinear ordinary differential equation for $h(t)$ that can be solved numerically (Hoggan 1997).

Computational Analysis

The watershed centroidal lag is estimated in the computational implementation of the model by using the empirical equation inferred by the California Highways and Public Works (Miller and Clark 1960):

$$T^* = 0.95 \cdot \left(\frac{L^3}{H}\right)^{0.385} \tag{23}$$

where L = length of the longest watercourse in kilometers (i.e., the distance between Points A and B along the stream in Fig. 1); H = elevation difference (between the same Points A and B in Fig. 1) in meters; and T^* is obtained in hours.

To be specific, a typical watershed was selected to conduct the parametric studies in this investigation (de Béjar 2001). The sample watershed-reservoir-dam system is located in Zone 7, east of the 105° meridian. The basin area measures 160 km^2, and the longest course is 30 km, with an elevation difference of 120 m. The local hydrologic soil-cover complex number (S) is derived from an estimated SCS curve number of 65, and the deterministic 6-h point PMP is stipulated as 65 cm of rain.

The selected site is assumed in Peoria County, Illinois, with antecedent moisture condition Type II, which takes the soil moisture supply within the watershed to be similar to the average conditions just before the occurrence of the maximum annual flood (Miller and Clark 1960). Maps of local soil series indicate that over 50% of the area is composed of either Clinton or Carrington soils; therefore, in terms of the relative infiltration rate, the watershed soil is considered SCS Group B. The local usage is composed of (1) row crops (45%); leading to an SCS curve number of 75; (2) legumes (35%), leading to an SCS curve number of 69; and (3) pasture (20%), leading to an SCS curve number of 35. The resultant composite curve number is $0.45 \cdot (75) + 0.35 \cdot (69) + 0.20 \cdot (35) = 64.9$, say 65. The corresponding local hydrologic soil-cover complex number can be estimated as $S = 1{,}000/(\text{curve number}) - 10 = 1{,}000/65 - 10 = 5.39$, say 5.4.

The reservoir routing is characterized by the regression parameters $\alpha = 4{,}740$ m^3/m and $\beta = 35$ m^2/m, and the barrier spillway at its far end has an ogee at elevation $z = 90$ m and a weir length of 27 m. The parametric studies are based on variations, one parameter at a time, from this basic watershed-reservoir-dam system configuration.

Surface Hydrographs

Next, the watershed outflow hydrograph and the associated reservoir-pool hydrograph are generated for a drainage basin with a continuously varying centroidal lag. Figs. 6 and 7 show the resulting surface hydrographs for a rather severe design storm with PMP = 75 cm. Notice the pronounced peak of the hydrographs (i.e., of the trace of the corresponding surface on the plane

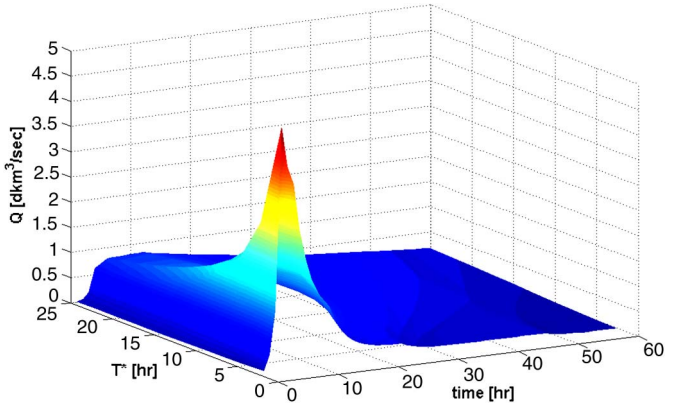

Fig. 6. Three-dimensional representation of a typical watershed outflow hydrograph surface (deterministic PMP = 75 cm)

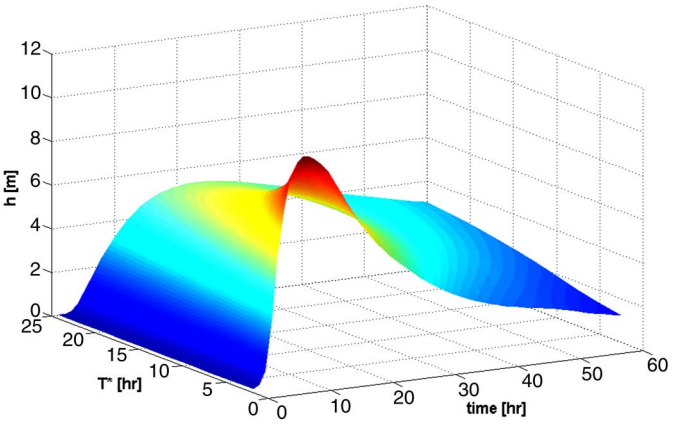

Fig. 7. Three-dimensional representation of a typical reservoir-pool hydrograph surface (deterministic PMP = 75 cm)

T^* = constant) for watersheds with rapid-evacuation characteristics (relatively short T^*) and the small residual quantity at the end of the response history. Watersheds with slow-evacuation characteristics (relatively long T^*) tend to remain flat in time, and therefore they show larger residual quantities at the end of the response history. Figs. 8 and 9 show these hydrographs for the selected design storm with PMP = 75 cm. The trends in the family of curves remain the same with smaller magnitudes of response associated with smaller design storms.

Similarly, hydrographs for watershed outflow and for the corresponding reservoir pool are built for the same watershed with the magnitude of the water-input event (PMP) ranging from 40–90 cm. Figs. 10 and 11 show sets of hydrograph families for a slow-evacuation watershed (T^* = 15 h). Both sets tend to support the basic assumption under the standard unit-graph superposition principle applied in practice that the response hydrographs essentially retain their shapes with the ordinates amplified in proportion to the magnitude of the water-input event.

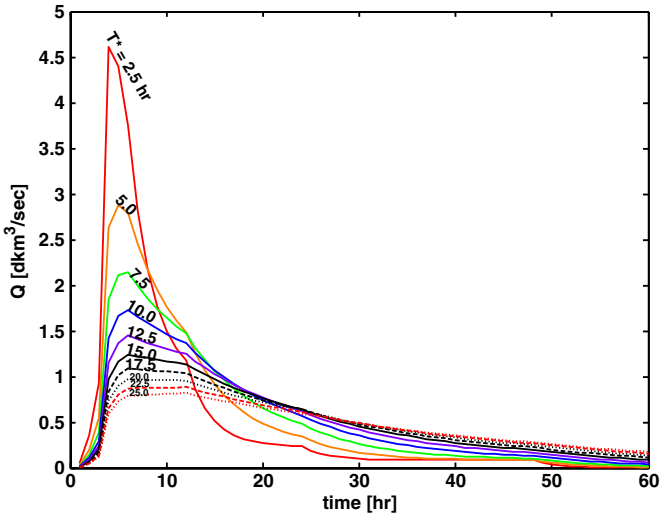

Fig. 8. Family of watershed outflow hydrographs (PMP = 75 cm, T^* variable)

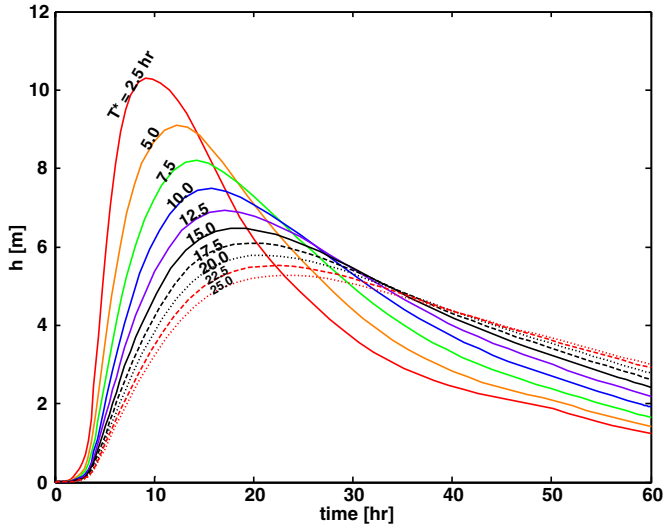

Fig. 9. Family of reservoir-pool hydrographs (PMP = 75 cm, T^* variable)

Response Spectra

The peak values of response in terms of the watershed outflow and the reservoir pool can be recorded for a continuous variation of the centroidal lag, with the magnitude of the water-input event as a parameter. The resulting family of curves constitutes the response spectra for the response quantity under consideration. Figs. 12 and 13 show the response spectra for the watershed outflow $Q(t)$ and the reservoir pool $h(t)$, respectively.

The set of response spectra for the watershed outflow is very sensitive to the particular order of the resulting aleatory permutation of the hourly storm precipitation values during the first 6 h of the water-input event. More unfavorable system responses are obtained when the largest incremental rain value occurs during the sixth storm hour than the responses for those storms in which the largest incremental rain value occurs during the first hour.

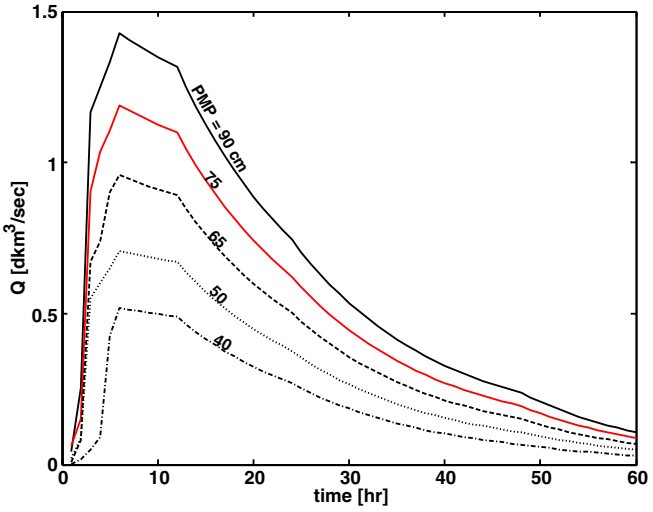

Fig. 10. Family of reservoir inflow-flood hydrographs (i.e., watershed outflow hydrographs) for a deterministic watershed with a relatively long centroidal lag time (T^* = 15 h) for several values of the water-input event PMP

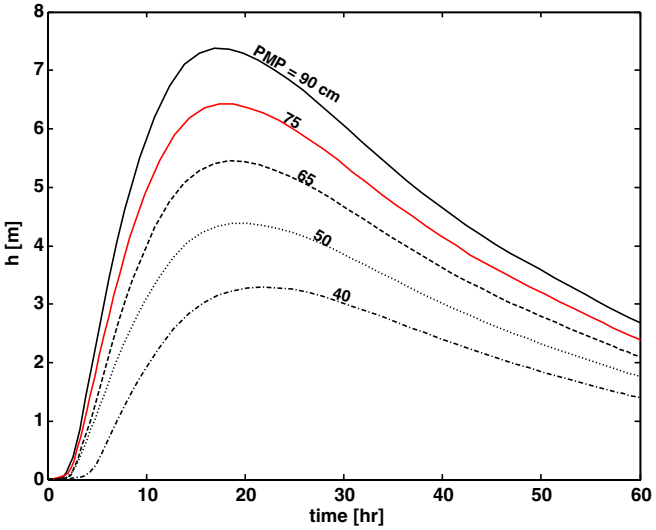

Fig. 11. Family of reservoir-pool hydrographs built for a deterministic watershed with a relatively long centroidal lag time (T^* = 15 h) for several values of the water-input event PMP

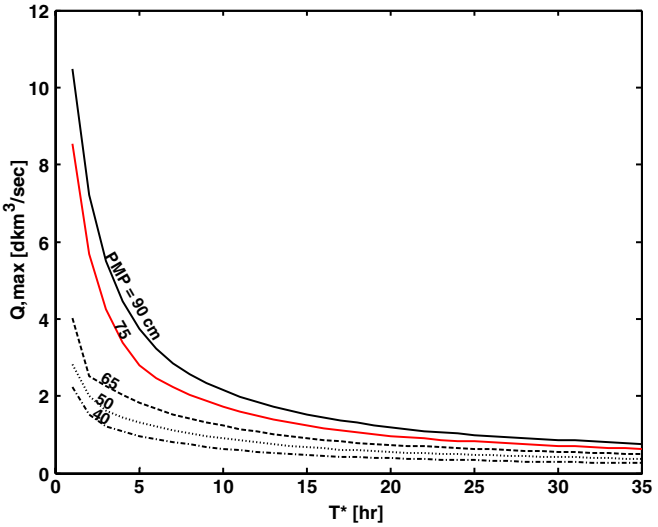

Fig. 12. Family of watershed outflow spectra for several values of the water-input event PMP

This sensitivity becomes apparent for the rapid-evacuation watersheds (those with relatively short T^*), as evidenced by the nonsmooth gradient of $Q_{,\max}$ with respect to the storm magnitude (PMP) in Fig. 12.

By contrast, the set of spectra for the reservoir pool exhibits relatively smooth transitions when the storm magnitude is varied. There are two fundamental reasons for this behavior: (1) the peak response of $h(t)$ for a given hydrograph systematically shows a delay with respect to the peak of $Q(t)$ (see Figs. 9 and 10), occurring at some time-distance of the particular hourly incremental rain lumps during the first 6 h of storm; and (2) the peak response of $h(t)$ occurs after a second filter in the system has acted on the water input to the watershed. The reservoir-pool spectra in Fig. 13 can be closely approximated by the following useful mathematical expression:

$$h_{,\max} = h_2(T^*) + \frac{[h_1(T^*) - h_2(T^*)]}{50.8} \cdot (\text{PMP} - 38), \quad \text{PMP} \geq 38 \tag{24}$$

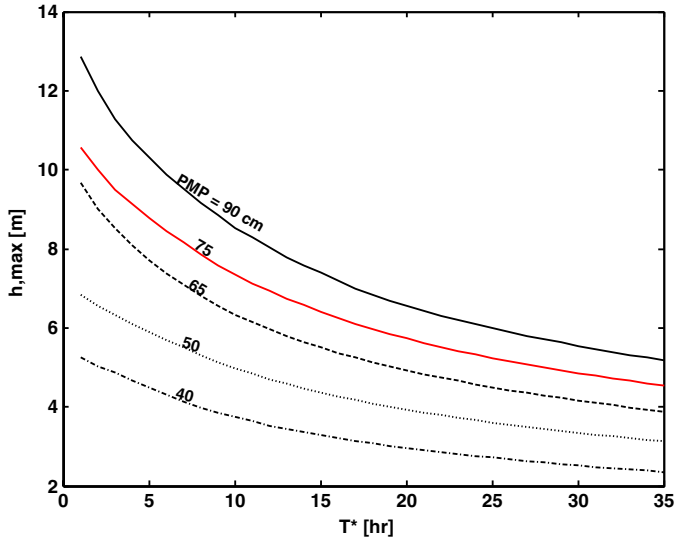

Fig. 13. Family of reservoir-pool spectra for several values of the water-input event PMP

where

$$h_1(T^*) = 14.375 - 2.566 \cdot \ln(T^*)$$

$$h_2(T^*) = 5.128 - 0.1583 \cdot (T^*) + 0.002263 \cdot (T^*)^2$$

and the PMP is given in centimeters of rain.

Residual Response

Similarly, the residual values of response in terms of the watershed outflow and the reservoir pool at the end of the observed history can be recorded and represented graphically, as in Figs. 14 and 15, respectively. The recorded values take place at a far time-distance of the local rain distribution during the first six storm hours, and the resulting curves exhibit smooth gradients with the magnitude of the water-input event. The watershed residual outflow in Fig. 14 can be closely approximated by the following mathematical expression:

$$Q_{,\text{res}} = Q_{r2}(T^*) + \frac{[Q_{r1}(T^*) - Q_{r2}(T^*)]}{50.8} \cdot (\text{PMP} - 38), \quad \text{PMP} \geq 38 \tag{25}$$

where

$$Q_{r1}(T^*) = -18.6213 + 3.5508 \cdot T^* + 0.4670 \cdot (T^*)^2 - 0.00976 \cdot (T^*)^3$$

$$Q_{r2}(T^*) = -1.7401 - 0.4169 \cdot T^* + 0.2275 \cdot (T^*)^2 - 0.00422 \cdot (T^*)^3$$

and the PMP is given in centimeters of rain.

Likewise, the reservoir residual pool in Fig. 15 can be closely approximated by the following mathematical expression:

$$h_{,\text{res}} = h_{r2}(T^*) + \frac{[h_{r1}(T^*) - h_{r2}(T^*)]}{50.8} \cdot (\text{PMP} - 38), \quad \text{PMP} \geq 38 \tag{26}$$

where

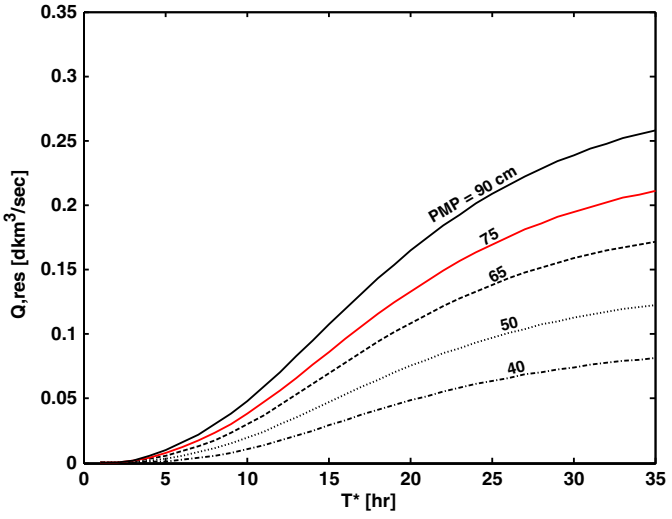

Fig. 14. Family of residual watershed outflows at the end of the considered history ($t = 60$ h) for several values of the water-input event PMP

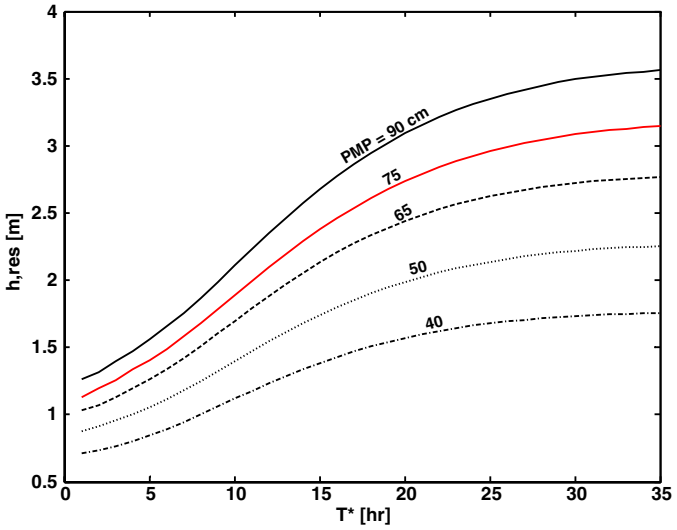

Fig. 15. Family of residual reservoir pools at the end of the considered history ($t = 60$ h) for several values of the water-input event PMP

$$h_{r1}(T^*) = 1.0613 + 0.1088 \cdot T^* + 4.76 \cdot (10^{-4}) \cdot (T^*)^2 - 4.427 \cdot (10^{-5}) \cdot (T^*)^3$$

$$h_{r2} = 0.5857 + 0.0628 \cdot T^* - 5.4055 \cdot (10^{-4}) \cdot (T^*)^2 - 8.77 \cdot (10^{-6}) \cdot (T^*)^3$$

Probabilistic Model

Instantaneous Response Distributions

Next, two fundamental variables into the routing of the water-input event through the watershed-reservoir-dam system, namely, the storm magnitude and the watershed centroidal lag, are assumed random. The 6-h point storm magnitude is modeled with the extreme-value distribution Type I, of the largest values (Gumbel distribution), with mean value given by the deterministic assessment of the 6-h point PMP (Miller and Clark 1960; USBR 1976, 1977), and with a coefficient of variation estimated as 0.1. The watershed centroidal lag is assumed lognormally distributed, with mean value given by the deterministic assessment and with a coefficient of variation estimated as 0.3. The objective in this investigation is to identify the instantaneous distribution of the response hydrograph for the reservoir pool, $h(t)$, because this random process represents the effective hazard on the dam (de Béjar 1999). Sampling is conducted on the basis of Monte Carlo simulations (Benjamin and Cornell 1970; Soong and Grigoriu 1993).

Ten thousand simulations were conducted on the basic watershed-reservoir-dam system, allowing both the storm magnitude and the watershed centroidal lag to assume random realizations. Subsequently, the variates for the reservoir pool at times $t = 12$ h and $t = 24$ h and the peak value of the reservoir pool regardless of the time of occurrence were examined. On the basis of exploratory statistical analysis of the data generated for these three variates (MathSoft 1999; de Béjar 2001), it was concluded that the best fit was provided by the lognormal distribution, which fit the data accurately and has sufficient simplicity for engineering applications. However, the normal distribution also produced satisfactory goodness-of-fit to the data, and therefore, flood hazard curves were produced separately on both assumptions, a lognormal and a normal pool random process $h(t)$, for comparison.

To generate the probability density function of the pool response $h(t^*)$ at time t^*, 1,000 simulations were conducted, and the sample coefficient of variation of the variate $h(t^*)$ was inferred from the data. The mean value of $h(t^*)$ was calculated from the deterministic model by using the stipulated mean values of the storm magnitude and the watershed centroidal lag. This second-moment characterization of the variate completely defines the postulated underlying distribution, whether lognormal or normal. Correspondingly, similar calculations for the variate peak value in the watershed response history $h(t)$, regardless of the time of occurrence, produced sample estimations for the second-moment characterization of the maximum value of $h(t)$, which completely defines the postulated underlying distribution. The desired hazard curve is given by the associated complementary probability distribution function (Benjamin and Cornell 1970).

Noise in the Reservoir

Consider that the bottom of the reservoir may be randomly covered with sediments over time; that topographical surveys are imperfect, particularly in the vicinity of the boundary of the reservoir; or that the actual values of the regression coefficients α and β for the gradient of reservoir storage with changes in reservoir pool may deviate randomly from the theoretical estimations. The influence of these factors on the reservoir response can be modeled by including a Gaussian noise term in the governing differential equation for the reservoir (Jiang 1998). The result of such formulation is equivalent to adding to the reservoir-pool response obtained previously [upon solving Eq. (19)] the contribution to the response from the Gaussian noise term, $\hbar(t)$, which is governed by the following zero-initial-condition Itō stochastic differential equation (Larson and Shubert 1979; Soong and Grigoriu 1993):

$$\frac{d\hbar(t)}{dt} = \frac{\sigma}{G[h(t)]} \cdot \frac{dW_0(t)}{dt} \tag{27}$$

where $h(t)$ = total reservoir-pool response (including the contribution from the noise); $dW_0(t)/dt$ = white Gaussian noise; and σ = noise intensity. This expression may also be written as the following special case of the Langevin's equation:

$$d\hbar(t) = \frac{\sigma}{G[h(t)]} \cdot dW_0(t) \tag{28}$$

where W_0 = standard Wiener process. The solution for this unpredictable noise is given by the following Wiener integral:

$$\hbar(t) = \sigma \cdot \int_0^t \frac{dW_0(\tau)}{G[h(\tau)]} \tag{29}$$

which may be expressed in discrete form for numerical calculations as the following Itō summation:

$$\hbar(t_i) = \sigma \cdot \sum_{t_k=0}^{t_i-\Delta t} \frac{1}{\alpha + \beta \cdot h(t_k)} \cdot \Delta W_0(t_k) \tag{30}$$

where $\Delta W_0(t_k) = W_0(t_{k+1}) - W_0(t_k)$ = zero-mean Gaussian process with variance $\Delta t_k = t_{k+1} - t_k = \Delta t$; and Δt = time step.

The empirical value of the noise intensity, σ, must be identified for the specific reservoir under study, and it is arbitrarily taken as $\sigma = 1$ dkm^3·s$^{-1/2}$ for numerical calculations in this investigation.

Fig. 16 shows the mean function for the reservoir pool assumed to be given by the deterministic response hydrograph for the watershed-reservoir-dam system with the input data described previously. The evolution of the corresponding response random process assumed as lognormally distributed is also shown in Fig. 16. Generally, as time increases along the recession limb, there is less dispersion in the prediction because the response variances decrease. The pool response to the water-input event with noise in the reservoir is included in the figure for comparison with the corresponding response without noise. In general, the presence of the noise increases the dispersion of the response random process under consideration. Fig. 17 shows the flood hazard curve for the reservoir pool with and without noise in the reservoir, assuming that the response random process is lognormally distributed. The noise causes the hazard to increase substantially. For example, given that the crest of the nonoverflow section is approximately 9.2 m above the level of the spillway crest, the probability of overtopping turns out to be 6.2% for a noisy reservoir, as compared to 2.4% for an ideal reservoir. Figs. 18 and 19 show a parallel development for the pool and the associated flood hazard curve, respectively, assuming that the reservoir-pool response process is normally distributed. Now the probability of overtopping is 4.5% for a noisy reservoir, as compared to 1.0% for an ideal reservoir.

In general, the magnitude of the hazard is increased when the response processes as taken as lognormally distributed, as compared to the results with the normal assumption. The lognormal assumption for the response process proved accurate in this investigation for the probabilistic simulation of routing of a water-input event through a watershed-reservoir-dam system. Therefore, the

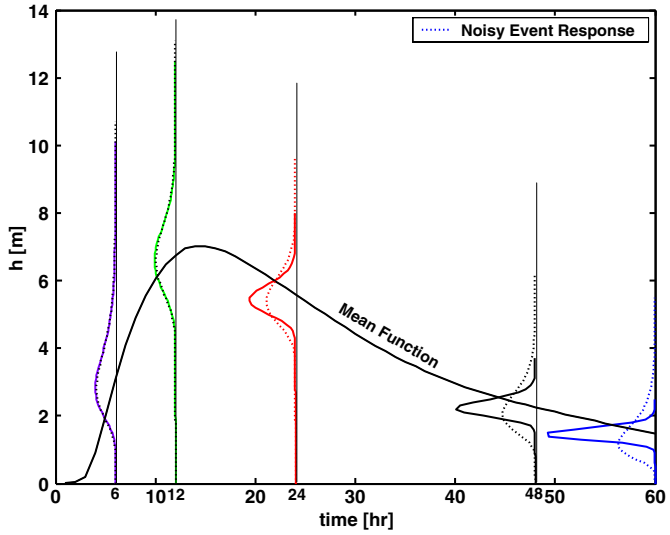

Fig. 16. Mean function of the reservoir pool and schematic representation of the random process $h(t)$, assumed lognormal, with and without noise in the reservoir (for clarity, evolving probability density functions appear amplified by a factor 5.0)

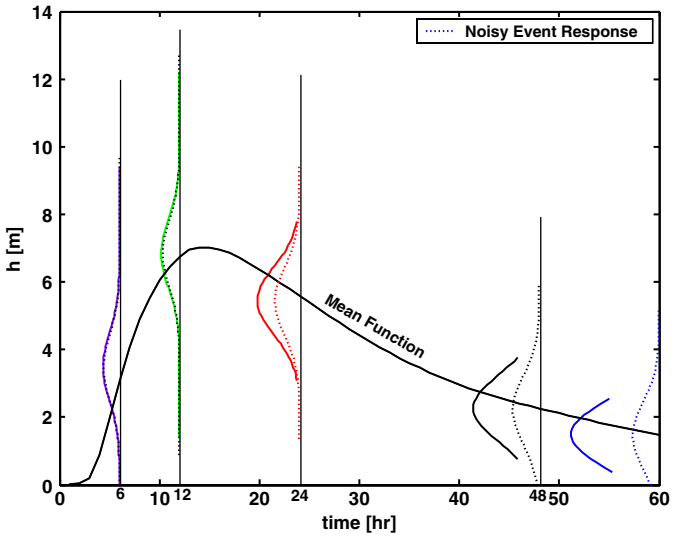

Fig. 18. Mean function of the reservoir pool and schematic representation of the random process $h(t)$, assumed normal, with and without noise in the reservoir (for clarity, evolving probability density functions appear amplified by a factor 5.0)

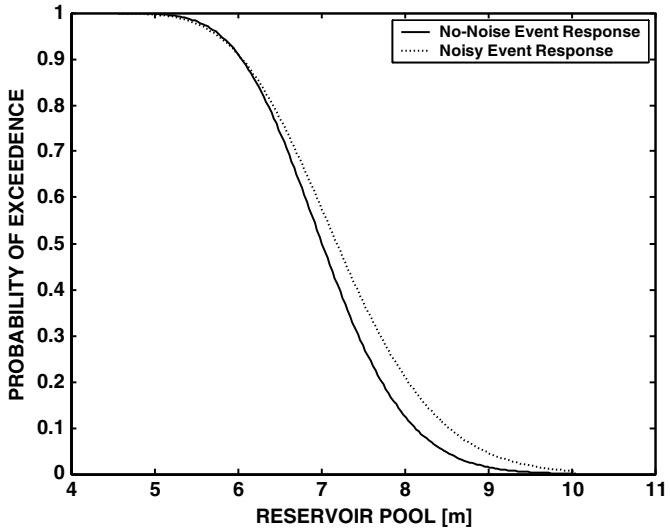

Fig. 17. Flood hazard curve for the random process $h(t)$, assumed lognormal, with and without noise in the reservoir

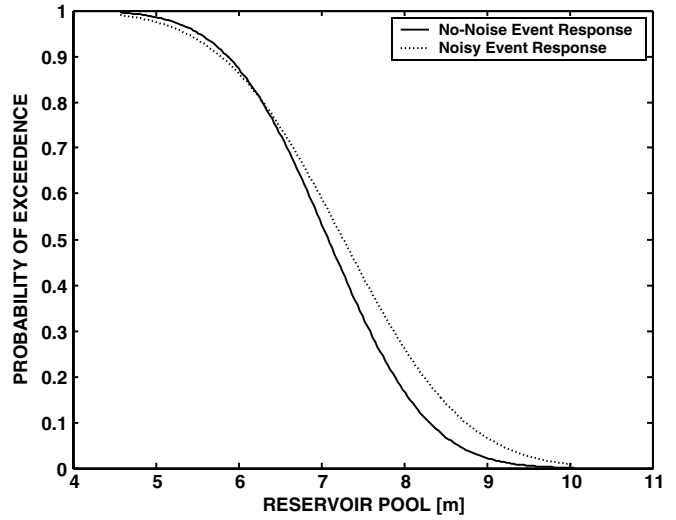

Fig. 19. Flood hazard curve for the random process $h(t)$, assumed normal, with and without noise in the reservoir

use of the lognormal distribution is recommended for practical applications to real systems in the field.

Conclusions

The following conclusions are derived from this investigation:

1. A rational theoretical model was developed to represent the routing of a water-input event through a watershed-reservoir-dam system and to assess its response in terms of the inflow design flood into the reservoir and the resulting reservoir pool. However, the model includes various simplifications to allow for mathematical tractability, and the values of several parameters required in the parametric study were simply postulated at this time.
2. Both deterministic and probabilistic implementations of the model allow ready computational analysis useful for design and for situational assessment.
3. At this time, the random processes for the overall system response appear to be best modeled as lognormally distributed. However, although the methodology developed in this investigation is solid, mutual validation may force the evolution of specific probabilistic models as more information becomes available.
4. Noise in the reservoir component is easily included in the probabilistic formulation of the model and has an important influence in the magnitude of the resulting hazard. This is an innovative contribution of this study. An accurate assessment of the noise intensity may prove difficult in practice, but realistic reliability assessments can be conducted using bounds on the noise intensity.
5. The model provides direct evaluation of the probability of overtopping in a given flood scenario and provides the fundamental hazard curve for complete risk analysis of the dam structure, including the possible sliding, overstressing, and overturning modes of failure.

Acknowledgments

This investigation was conducted under the work unit "Failure Mechanisms of Concrete Dams" of the Risk Analysis for Dam Safety Research Program, part of the Research Program on Civil Works sponsored by the Department of the Army, Corps of Engineers, Headquarters. The author gratefully acknowledges the support and guidance provided by the Office of the Chief of Engineers and by the Army Engineer District representatives in the Field Review Group. Approved for public release; distribution is unlimited. Permission to publish was granted by the Director of the Geotechnical and Structures Laboratory, U.S. Army Engineer Research and Development Center.

Notation

The following symbols are used in this paper:

A, B = end points of the longest reach in the drainage basin under consideration;
a_i, b_i = empirical coefficients;
b = weir length;
C = constant of integration;
c = discharge coefficient;
dkm^3 = $\mathrm{km}^3/10$;
d/dt = time derivative;
$G[h(t)]$ = reservoir storage expressed as a function of the reservoir pool;
H = elevation difference between the end Points A and B;
$h(t)$ = reservoir-pool response defined as the reservoir water level over the spillway crest;
$h_{,\max}$ = maximum value of the reservoir pool;
$h_{,\mathrm{res}}$ = residual reservoir pool;
$h_{ri}(T^*)_{,i=1,2}$ = auxiliary functions of T^*;
h_1, h_2 = auxiliary functions of T^*;
$\hbar(t)$ = Gaussian noise component of the reservoir pool response $h(t)$;
I_a = initial abstraction;
i = index;
k^* = reciprocal of T^*;
L = length in kilometers of the longest watercourse in the watershed (equivalent to L_r expressed in kilometers);
L_r = length of the longest reach in the drainage basin;
PMP = probable maximum precipitation;
p_i = accumulative runoff at the end of the ith time interval;
p_i^* = recalculated value of p_i after considering a physical lower bound for the hourly loss during the ith time interval;
$Q(t)$ = inflow to the reservoir; i.e., the response of the watershed to the water-input event;
$Q_{,\max}$ = maximum value of the watershed outflow;
$Q_{,\mathrm{res}}$ = residual value of the watershed outflow;
$Q_{ri}(T^*)_{,i=1,2}$ = auxiliary polynomial functions of T^*;
$q(t)$ = watershed flow response;
$q[h(t), c]$ = spillway outflow as a function of the reservoir pool response $h(t)$ and the discharge coefficient c;
q_{pk} = maximum value of the reservoir outflow;
$r(t)$ = rate of rain;
r_i = accumulative rainfall in the actual-size watershed at the end of the ith time interval;
S = local hydrologic soil-cover complex number;
$S(t)$ = watershed storage;
T^* = centroidal lag between the inflow and outflow hydrographs;
t = time;
t_w = termination time of the water-input event;
U_W = velocity of propagation of the flood wave;
$u(t)$ = unit-impulse response function;
$W_o(t)$ = standard Wiener process;
z = weir elevation;
α, β = empirical coefficients;
Δ = increment symbol;
ΔL_i = loss corresponding to the ith time interval;
$\delta(t)$ = Dirac delta function applied at the origin of time;
ε = infinitesimal time interval;
$\sum$ = summation symbol;
σ = noise intensity; and
ω_o = inflow magnitude.

References

Benjamin, J. R., and Cornell, C. A. (1970). *Probability, statistics, and decision for civil engineers*, McGraw-Hill, New York.

de Béjar, L. A. (1999). "Fragility analysis of concrete gravity dam safety under flood." *Proc., Dam Safety*, Association of State Dam Safety Officials, Lexington, KY.

de Béjar, L. A. (2001). "Convex watershed-reservoir model for risk assessment of spillways and non-overflow dam monoliths subjected to flood hazard." *Technical Rep. ERDC/GSL TR-01-8*, U.S. Army Engineer Research and Development Center, Vicksburg, MS.

Dingman, S. L. (1994). *Physical hydrology*, Macmillan, New York.

Ellingwood, B. R. (1995). "Engineering reliability and risk analysis for water resources investments; role of structural degradation in time-dependent reliability analysis." *ITL Rep. 95-3*, U.S. Army Corps of Engineers Waterways Experiment Station, Vicksburg, MS.

Hoggan, D. H. (1997). *Computer-assisted hydrology and hydraulics*, 2nd Ed., McGraw-Hill, New York.

Jiang, S. (1998). "Application of stochastic differential equations in risk assessment for flood releases." *Hydrol. Sci. J.*, 43(3), 349–360.

Larson, H. J., and Shubert, B. O. (1979). *Probabilistic methods in engineering sciences: Random noise, signals, and dynamic systems*, Vol. 2, Wiley, New York.

MathSoft. (1999). *S-plus 2000: Modern statistics and advanced graphics*, Seattle.

Miller, D. L., and Clark, R. A. (1960). "Flood studies." *Design of small dams*, 1st Ed., U.S. Dept. of the Interior, Bureau of Reclamation, Denver.

Olson, R. M. (1961). *Engineering fluid mechanics*, International Textbook, Scranton, PA.

Soong, T. T., and Grigoriu, M. (1993). *Random vibration of mechanical and structural systems*, Prentice-Hall, Englewood Cliffs, NJ.

Street, R. L., Watters, G. Z., and Vennard, J. K. (1996). *Elementary fluid mechanics*, 7th Ed., Wiley, New York.

U.S. Bureau of Reclamation. (1976). "Inflow design flood studies." Appendix G, *Design of gravity dams*, Dept. of the Interior, Denver.

U.S. Bureau of Reclamation. (1977). "Inflow design flood studies." Appendix L, *Design of arch dams*, Dept. of the Interior, Denver.

Queries

1. Please provide 10 mi^2 in SI units.
2. The double parentheses in the spillway outflow have been changed to square brackets as per ASCE style. Please confirm if this change is acceptable.
3. Please carefully check each figure and caption to ensure each is accurate.